This paper has been selected in Materials Science Forum, Vols.546-549, 2007, pp1319-1326.

Quantification of High Temperature Strength of Nickel-based Superalloys

Zhanli Guo, N. Saunders, A.P. Miodownik and J-Ph. Schillé

[1]Sente Software Ltd., Surrey Technology Centre, Guildford GU2 7YG, U.K.

[a] z.guo@sentesoftware.co.uk

Keywords: Nickel-based superalloys; Strengthening; Precipitation hardening; Creep; Modelling

Abstract. The strength of nickel-based superalloys usually consists of solid solution strengthening from the gamma matrix and precipitation hardening due to the gamma' and/or gamma" precipitates. In the present work, a model was developed to calculate the high temperature strength of nickel-based superalloys, where the temperature dependence of each strengthening contribution was accounted for separately. The high temperature strength of these alloys is not only a function of microstructural changes in the material, but the result of a competition between two deformation modes, i.e. the normal low to mid temperature tensile deformation and deformation via a creep mode. Extensive validation had been carried out during the model development. Good agreement between calculated and experimental results has been achieved for a wide range of nickel-based superalloys, including solid solution alloys and precipitation-hardened alloys with different type/amount of precipitates. This model has been applied to two newly developed superalloys and is proved to be able to make predictions to within useful accuracy.

1. Introduction

Nickel-based superalloys have been widely used in aircraft engines and land-based gas turbines where high strength at elevated temperatures is required. It has always been an important task to develop alloys with better high temperature properties. Improved properties may be achieved by modifying alloy chemistry and processing route. Traditionally, alloy design follows a trial-and-error approach which is both costly and time consuming. It is now highly desirable to develop advanced computer models to facilitate the design of alloy composition and processing route.

The strength of nickel-based superalloys arises from solid solution strengthening in the γ matrix and precipitation hardening due to the ordered γ' precipitates which are coherently embedded in the matrix. When temperature increases, both strength contributions will be affected, resulting in a change in the alloy's strength. In the present work, a computer model has been developed such that the strength of nickel-based superalloys can be calculated as a function of alloy composition, heat treatment and temperature. The model is based on general theories on phase transformations (including thermodynamics and kinetics) and strengthening, and is therefore able to perform calculations in a predictive manner to within useful accuracy. Recently a similar attempt was made by Nembach and co-workers.[1] However, their model only dealt with two alloys and many important material parameters, set as constants, were obtained by fitting calculation with experimental results for each alloy. Since in reality the values of these parameters differ from alloy to alloy, such model has little predictive capacity.

In the first part of the paper, the procedures for developing the model are described in detail. The second part features validation of the model over a wide range of commercial alloys including solid solution alloys and precipitation-hardened alloys with different type/amount of precipitates. The model was then applied to two newly developed nickel-based superalloys. The model for high temperature strength calculation forms part of the development of a computer software, *JMatPro*, which allows the present calculations to be carried out readily via a user-friendly graphical interface.

2. Model Development

The first step of the model development is to calculate solid solution strengthening and precipitate hardening at room temperature (RT). The influence of temperature on each contribution will then be discussed. When the temperature is high enough, the alloy will deform via a creep mechanism. Therefore the creep behaviour of nickel-based superalloys is also discussed.

2.1 Solid Solution Strengthening. The yield stress σ_y of a single phase material is calculated using the standard Hall-Petch equation:

$$\sigma_y = \sigma_{y0} + k d_g^{-1/2} \quad (1)$$

where σ_{y0} and k are the intrinsic flow stress and Hall-Petch coefficient of that phase both of which are composition dependent, and d_g is the grain size. Accurate information on phase fractions and constituents is obtained from thermodynamic calculations within JMatPro, the reliability of which has been extensively tested.[2,3] Eq. 1 draws on a flow stress database and a Hall-Petch coefficient database to describe the composition dependence of σ_{y0} and k in a single phase, based on work from literature.[4,5,6,7] These databases have been validated on numerous solid solution nickel-based alloys and stainless steels.[8,9] Comparison between the calculated and experimental results is shown in Fig. 1. It should be noted that the same equation and data can be used to calculate the yield stress of the face-centred-cubic (FCC) phase in both nickel-based superalloys and steels.

Once accurate calculations are available for the room temperature strength (σ_{RT}) of an alloy, the next step is to relate the strength at high temperature to this room temperature value. Examination of the yield strength as a function of temperature, $\sigma(T)$, for many austenitic steels and nickel-based solid solution alloys shows a clear correlation between the rate of decrease in $\sigma(T)$ with increasing temperature and σ_{RT}. The decay is well matched by an exponential equation of the following type:

$$\sigma(T) = \alpha + \beta \exp\left(\frac{-Q}{RT}\right) \quad (2)$$

where α and β are constants directly related to σ_{RT} and the value of Q, which is determined empirically through regression analysis based on the data of a wide range of austenitic steels and nickel-based solid solution alloys. The relationship between strength and temperature is well represented by Eq. 2, as shown in Fig. 2. It should be noted that strength data at temperature higher than 750°C were not included, for reasons that are discussed in later sections.

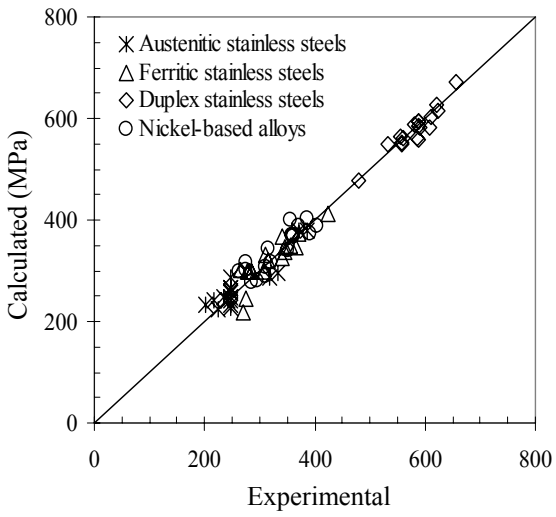

Fig. 1. Comparison between calculated and experimental yield strength at room temperature for solution hardening alloys

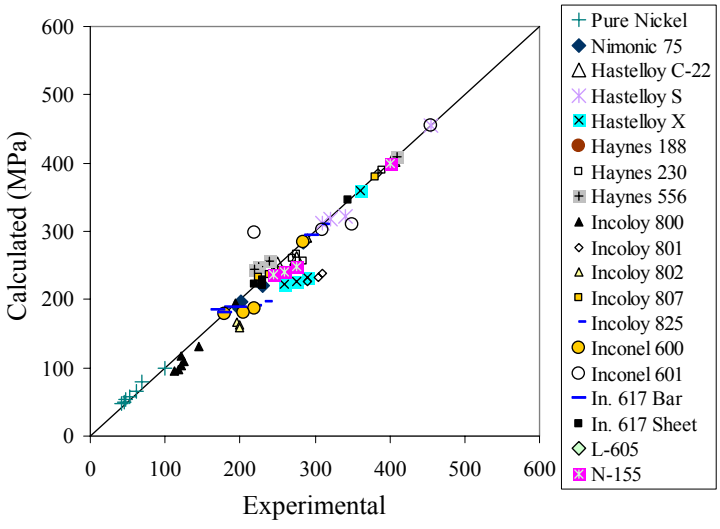

Fig. 2. Comparison between calculated and experimental yield strength over a wide temperature range for solution hardening nickel alloys

2.2 Precipitation Hardening. In nickel-based superalloys strengthened by ordered γ′ precipitates, dislocations with Burgers vector a/2<110> (a is the lattice parameter of the matrix) typically travel in pairs, because the passage of a pair of the matrix dislocations through a γ′ particle restores perfect order on the {111} slip plane. When the particle is small, the yield strength is determined by the strength that is necessary to move weakly coupled dislocation pairs. The first dislocation bows out and the second dislocation remains straight. The yield strength due to precipitation, σ_{y1}, can be expressed as:[10,11]

$$\sigma_{y1} = M\frac{\Gamma}{2b}[A_1(\frac{\Gamma f d}{T_l})^{1/2} - f] \quad (3)$$

where M is the Taylor factor that relates the yield strength in polycrystalline material and critical resolved shear strength in single crystal specimens (≈3 for FCC metals);[12] Γ is the antiphase boundary (APB) energy in the {111} plane; b is the Burgers vector of dislocation; d is the mean particle diameter; f is the volume fraction of the γ′ precipitates; T_l is the dislocation line tension, $Gb^2/2$, where G is the shear modulus of the matrix; and A_1 is a numerical factor depending on the morphology of the particles, which equals to 0.72 for spherical particles.

When particles become large, the coupling of the dislocations in the pair will be strong and both dislocations may reside in the same particle. Hüther and Reppich analysed this situation for spherical ordered precipitates and derived a formula in which the yield strength due to precipitation hardening is calculated as a function of the particle size according to:[13]

$$\sigma_{y2} = 1.72M\frac{T_l\omega f^{1/2}}{2bd}(1.28\frac{\Gamma d}{\omega T_l} - 1)^{1/2} \quad (4)$$

The parameter ω accounts for the repulsion of the dislocations within the precipitates, which is of the order of the unity and can be empirically determined.[14]

For any given particle size, the yield strength is governed by the lower of the two values, σ_{y1} and σ_{y2}, since dislocations always tend to move by whichever mechanism that provides the least resistance to glide. Most of the input into Eqs. 3 and 4 can be calculated through an equilibrium thermodynamic calculation combined with assessed databases for moduli and solid solution strengthening. The most critical factor was found to be the APB energy, which is obtained from a thermodynamic calculation route described previously.[15]

Calculations have been made for a number of commercial superalloys where detailed information on γ' particle size is available, Fig. 3. When size distributions are bi-modal or higher order, the amount of γ' at the final heat treatment temperature has been used for the calculation and the total strength was obtained by a simple summation of the strengthening effect from the various size fractions.[16,17]

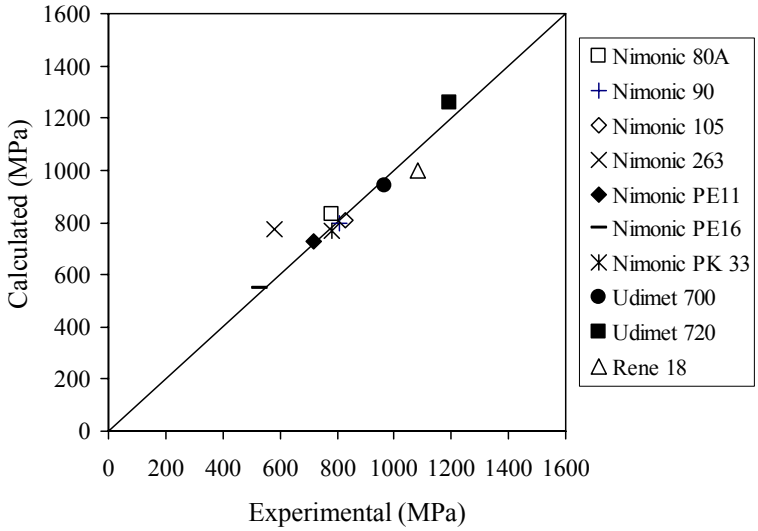

Fig. 3. Comparison between calculated and experimental yield strength for a series of commercial nickel-based superalloys with precipitation hardening

Alloys such as 625 and 718 are predominantly strengthened by γ" phase; same amount of γ" will provide substantially more strength than γ' owing to the significant lattice mismatch of γ" along its major axis, which provides a further strain hardening contribution.

For small γ" precipitates, the following equation is used to take this into account after Oblak et al.:[18]

$$\sigma_{\varepsilon 1} = 1.7 G \varepsilon^{3/2} \left(\frac{rf}{b} \right)^{1/2} \quad (5)$$

where $\sigma_{\varepsilon 1}$ is the strength contribution from strain hardening, ε is the lattice mismatch in the major axis,[19] r is the average radius of the particles in the major axis and f is the volume fraction of the particle. For large γ" precipitates, the strength contribution from strain hardening, $\sigma_{\varepsilon 2}$, is calculated using the following equation after Smallman:[20]

$$\sigma_{\varepsilon 2} = 0.7 G f^{1/2} \varepsilon^{1/4} \left(\frac{b}{r} \right)^{3/4} \quad (6)$$

The total particle strengthening contribution is considered to be a summation of that from strain hardening and dislocation cutting mechanisms. Based on the method described above, calculations have been made for the room temperature yield strength of a 718 alloy based on a γ grain size of 100 μm and γ' and γ" particle sizes of 15 and 25 nm respectively, taken from Chaturvedi and Han,[21] which is consistent with other studies of 718 and variants.[22,23] The yield strength is calculated as 1223 MPa, which falls in the range of 1185-1365 MPa for commercial 718 alloys.

The contribution of precipitation hardening on the deformation strength at higher temperatures follows exactly the same equations described above, by considering the temperature dependence of all the parameters involved in Eqs. 3-6. Fig. 4 demonstrates the accuracy of JMatPro calculation on the Young's modulus for various wrought nickel-based alloys between room temperature and 870ºC, in comparison with experimental data.[24] The overall strength of an alloy at room temperature or high temperature is the summation of the contributions from solid solution strengthening and precipitation hardening. The yield strength calculated this way has been labelled the low to mid temperature (LMT) deformation strength, to distinguish it from the creep strength (see next section).

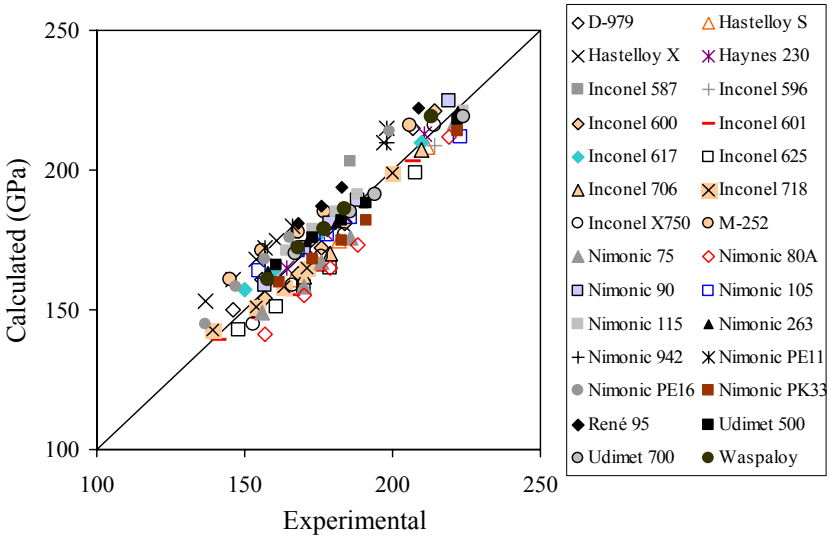

Fig. 4. Comparison between calculated and experimental Young's modulus over a wide temperature range for various wrought nickel-based superalloys

2.3 Creep Strength. When the temperature is over a critical temperature, which is typically around 800°C for nickel-based superalloys, there will be competition between yielding via the LMT deformation mechanism and creep at higher temperatures. In the latter case, the effective yield strength will then be the applied stress that is required to produce a creep rate equal to that strain rate used in the equivalent high temperature tensile testing. This critical value of the applied stress will be labelled the creep strength. The final yield strength of the material is whichever is the smaller value of the LMT deformation strength and the creep strength at the testing temperature.

Many formulations have been proposed to calculate the secondary creep rates,[25,26,27,28] however, there is as yet no relationship that can be considered as being universally applicable. The present work uses a formulation for the secondary creep rate [26] that features both a back stress function [29] and takes the stacking fault energy (γ_{SFE}) explicitly into account.[30] This approach was selected as it contains parameters that have an identifiable physical basis and which can be calculated self-consistently. The ruling equation is taken as:

$$\dot{\varepsilon} = A_2 D_{eff} \left[\frac{\gamma_{SFE}}{Gb}\right]^3 \left[\frac{\sigma - \sigma_b}{E}\right]^4 \quad (7)$$

where $\dot{\varepsilon}$ is the secondary creep rate, A_2 is a materials dependent parameter, D_{eff} is the effective diffusion coefficient, γ_{SFE} is the stacking fault energy of the matrix, σ_b is the back stress, E and G are the Young's modulus and Shear modulus of the matrix at the creep temperature, respectively. The back stress σ_b is calculated following the treatment of Lagneborg and Bergman.[28] D_{eff} is considered to have a contribution from pipe diffusion as well as lattice diffusion.[31,32] This becomes important at low temperature and high stress.

The majority of the input parameters in Eq. 7 can be obtained (or calculated) from databases already available within JMatPro.[33] The composition and amount of each phase such as γ, γ′ and/or γ″ at creep temperature are obtained from thermodynamic calculations. G and E are calculated from the physical property databases which include their temperature dependence. σ_b is directly calculated from the strengthening contribution of γ′ or γ″. γ_{SFE} at the creep temperature is calculated from the Gibbs energy difference between FCC and HCP structures,[34] and D_{eff} is calculated from the diffusion database. This leaves A_2 as the only adjustable parameter, whose value has been obtained by fitting calculations with experiments. Fig. 5 shows the correlation for a very wide range of alloys calculated using the approach described above. The experimental creep rates were drawn from literature.[21,35,36,37,38,39] As can be seen from Eq. 7, once the strain rate of the tensile test is known, the creep strength at this temperature for the same creep rate can be calculated.

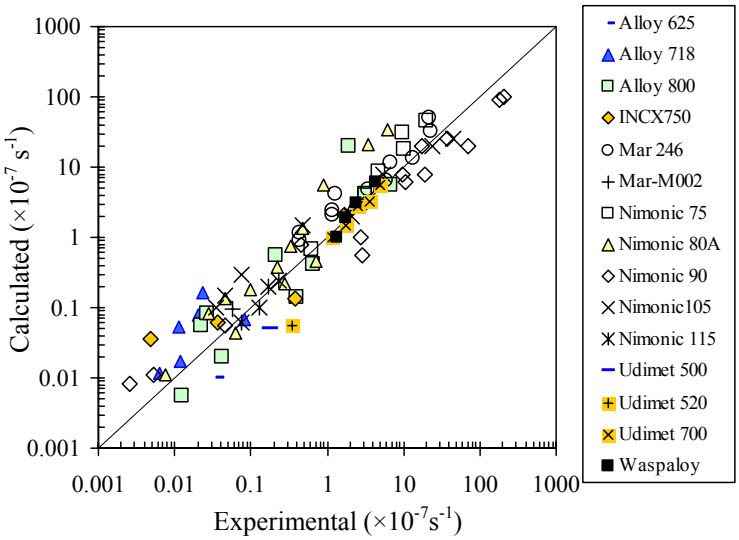

Fig. 5. Comparison between calculated and experimental secondary creep rate for Ni-based superalloys

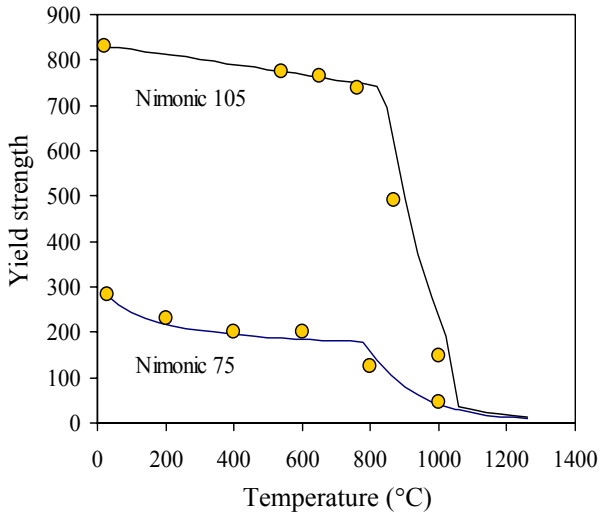

Fig. 6. Comparison between calculated and experimental high temperature yield strength of Nimonic 75 and Nimonic 105 alloys

3. Performance of the Model

Fig. 6 shows the comparison between experimental[40] and calculated yield strength vs. temperature for two commercial grades, one a solid solution alloy (Nimonic 75), the other hardened by γ′ precipitates (Nimonic 105). For Nimonic 105, in the creep controlled region, the alloy is weakened by the gradual removal of γ′ until it becomes fully γ above its solvus temperature of 1025ºC. The calculation procedure for solid solution alloys is simple as no phase changes take place. However, in the case of γ′ and γ" hardened alloys, the dissolution of both γ′ and γ" must be considered. Below the final heat treatment temperature, the amounts (and distributions) of γ′ and γ" are considered to be kinetically "frozen in" for the purposes of the calculation. Above this temperature dissolution to their equilibrium amount is allowed. The total number of γ′ and γ" particles is kept constant, which means

that they shrink in size with increasing temperature.

There are two ways to make the calculation for γ′ and γ" hardened alloys: (i) the size and distribution of particles after final heat treatment is used directly as the input; (ii) if this information is not known, the experimental yield strength can be used as an input and a single modal γ′ and/or γ" particle size back calculated to provide the requisite value for σ_{RT}. When γ′ and γ" coexist, a size ratio between γ′ and γ" particles is set arbitrarily as 2, close to experimental observations.[21]

Fig. 7 shows a comparison between calculated and experimental yield strength [40] for a variety of alloys from room temperature to high temperatures, where the measured σ_{RT} was used as input for the calculation. It can be seen that agreement is very good and the reduction in strength as a function of temperature is well matched.

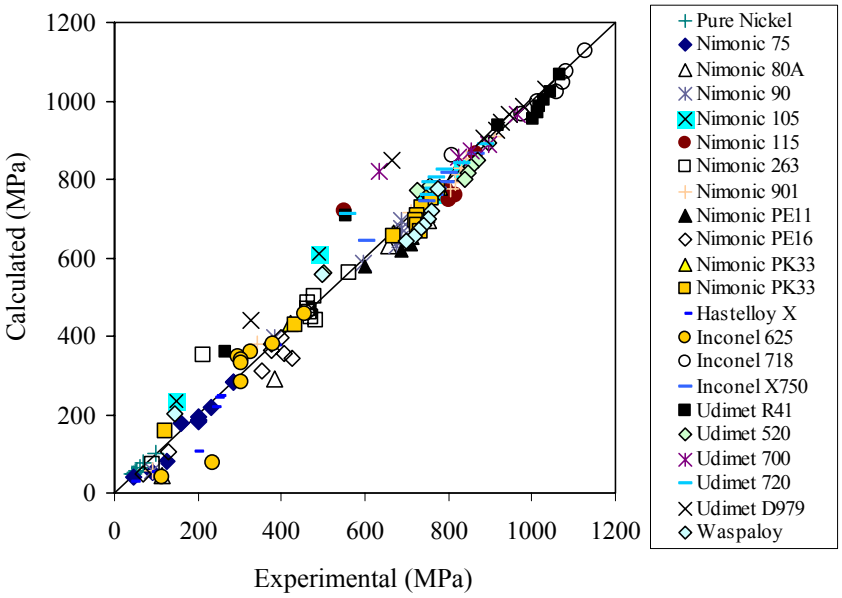

Fig. 7. Comparison between calculated and experimental high temperature strength of a wide range of commercial nickel-based superalloys

Recently, a new Ni-based superalloy, Inconel alloy 740 (Ni-24Cr-20Co-1Fe-0.5Mo-0.8Al-1.7Ti-2Nb-0.05C in wt%), has been designed to meet the demand for high efficiency in coal-fired power plants.[41] This alloy is strengthened by γ' formed during ageing at 800°C. Using the reported average grain size 50 μm and particle size 40 nm,[41] the room temperature yield strength of the alloy is calculated as 785 MPa. The strength vs. temperature curve based on this particle size is shown in Fig. 8. From the experimental yield strength vs. temperature curve in Ref. 41, the room temperature yield strength is estimated as 740 MPa and γ′ particle size back-calculated to be 53 nm. Using the room temperature yield strength 740 MPa as input, the strength vs. temperature curve was calculated and shown in Fig. 8.

Tancret et al. [42] designed a new Ni-based superalloy (Ni-20Cr-5Fe-2.3Al-2.1Ti-3.5W-0.4Si-0.07C-0.005B in wt%) for use in future fossil fuel power plant with steam temperatures as high as 750°C, with a composition. γ' precipitates form in this alloy during ageing treatment. Based on the experimental room temperature yield strength 790 MPa, the strength vs. temperature curve of this alloy was calculated and is shown in Fig. 9. Using the observed precipitate size 100 nm with a grain size of 175 μm, the calculated room temperature yield strength is 774 MPa and γ′ particle size back calculated to be 116 nm. The strength vs. temperature curve calculated based on this particle size is also shown in Fig. 9. A comparison has also been made between the calculated and experimental secondary creep rate, Table 1. The agreement is comparable with that obtained by the neural network technique used by Tancret but has the advantage that it is based on a more direct input of materials parameters rather than merely obtaining them from statistical analysis.

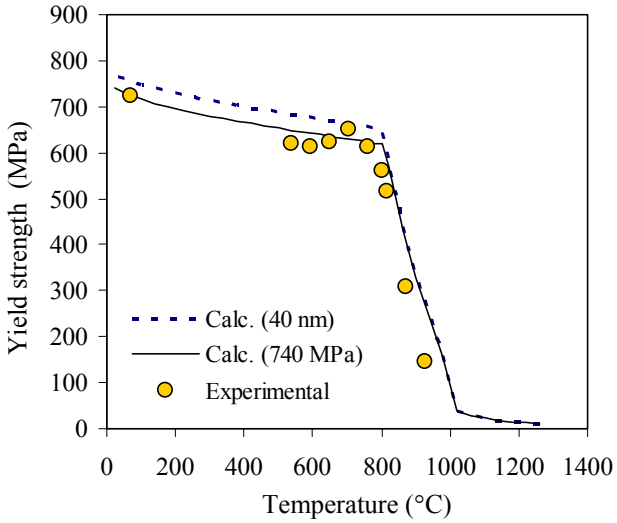

Fig. 8. Comparison between calculated and experimental high temperature yield strength of Inconel alloy 740

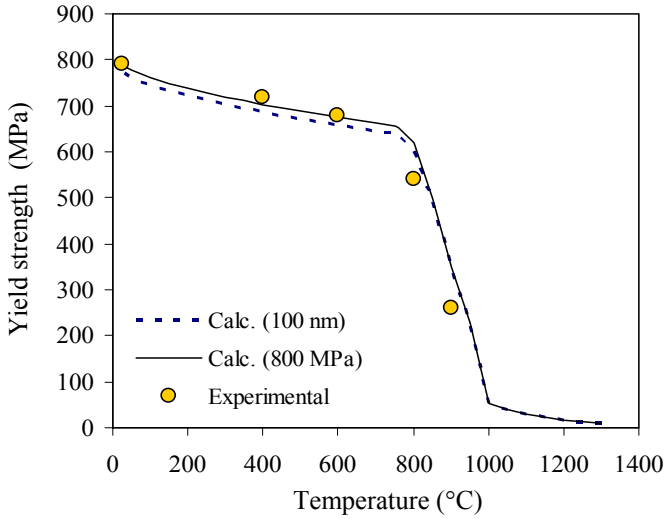

Fig. 9. Comparison between calculated and experimental high temperature yield strength of the alloy designed by Tancret et al.

Table 1. Comparison between experimental and calculated secondary creep rate at 750°C

Stress (MPa)	200	230	260	290	320
Exp. creep rate ($\times 10^{-9}$ s^{-1})	0.758	2.27	8.35	27.7	83.3
Cal. creep rate ($\times 10^{-9}$ s^{-1})	0.497	2.24	8.88	25.0	56.0

Summary

A model has been developed in the present work to calculate the high temperature strength of nickel-based superalloys, and includes the cross-over in deformation mechanisms attributable to low to mid temperature deformation and creep at higher temperatures. Good agreement between calculated and experimental results has been achieved for a variety of nickel-based superalloys, including solid solution alloys and precipitation-hardened alloys with different type/amount of precipitates. Extensive validations against experimental results were carried out during the development of the model. The model has been applied to two newly designed alloys and generated predictions in good agreement with experiments. A significant advantage of the present model is that all the information required for strength calculation can be obtained using materials parameters that are already present within existing JMatPro software and the implementation of the high temperature strength module can take advantage of the existing user-friendly interface.

References

1. E. Nembach, J. Pesicka, E. Langmaack, *Mater. Sci. Eng. A*, **A362** (2003) 264-273
2. X. Li, A.P. Miodownik, N. Saunders, *J. Phase Equilibria*, **22** (3) (2001) 247-253.
3. N. Saunders, S. Kucherenko, X. Li, A.P. Miodownik, J.P. Schillé, *J. Phase Equilibria*, **22** (4) (2001) 463-669.
4. F.B. Pickering, The Metallurgical Evolution of Stainless Steels: A Discriminative Section, ASM, The Metals Society, London, 1979, 1-42.
5. K.J. Irvine, T. Gladman, F.B. Pickering, *J. Iron Steel Inst.*, **207** (7) (1969) 1017-1028.
6. E.O. Hall, Yield Point Phenomena in Metals and Alloys, New York, Plenum, 1970
7. Y. Mishima, S. Ochiai, N. Hamao, M. Yodogawa, T. Suzuki, *Trans. Jpn. Inst. Met.*, **27** (9) (1986) 656-664.
8. X. Li, A.P. Miodownik, N. Saunders, *Mater.Sci.Technol.*, **18** (2002) 861-868.
9. N. Saunders, Z. Guo, X. Li, A.P. Miodownik, J.P. Schillé, *JOM*, **55** (12) (2003) 60-65
10. D. Raynor, J.M. Silcock, *Metal Science Journal*, **4** (1970) 121-130.

11. C.T. Sims, N.S. Stoloff, W.C. Hagel, Superalloys II, John Wiley & Sons, New York, 1987, 66-78.
12. B. Reppich, P. Schepp, G. Wehner, *Acta Metall.*, **30** (1982) 95-104.
13. W. Hüther, B. Reppich, *Z. Metallkde.*, **69** (1978) 628-634.
14. B. Reppich, *Acta Metall.*, **30** (1982) 87-94.
15. A.P. Miodownik, N. Saunders, in Applications of Thermodynamics in the Synthesis and Processing of Materials, eds. P. Nash and B. Sundman, Warrendale, PA: TMS, 1995, 91.
16. B. Reppich, W. Kühlein, G. Meyer, D. Puppel, M. Schulz, G. Schumann, *Mater. Sci. Eng.*, **83** (1986) 45.
17. D.J. Chellman, A.J. Luévano, A.J. Ardell, Strength of Metals and Alloys, London, Freund Publishing, 1991, 537.
18. J.M. Oblak, D.S. Duvall, D.F. Paulonis, *Mat. Sci. Eng.*, **13** (1974) 51.
19. C. Slama et al., *J. Mater. Res.*, **12**, 2299.
20. R.E. Smallman, Modern Physical Metallurgy, London, Butterworths, 1985, 392.
21. M.C. Chaturvedi, Y. Han, in Superalloy 718-Metallurgy and Applications, ed. E.A. Loria, Warrendale, PA, TMS, 1989, 489.
22. M. Sundararaman P. Mukhopadhyay and S. Banerjee, *Metall. Trans. A*, **23A** (1992) 2015.
23. E. Guo, F. Xu, E.A. Loria, in Superalloys 718,625 and Various Derivatives, ed. E.A. Loria, Warrendale, PA, TMS, 1991, 397.
24. *Adv. Mater. Proc.*, **156** (6) (1999) 80.
25. B. Wilshire, H.E. Evans, Creep of Metals and Alloys, Inst. Metals, 1985
26. X.S. Xie, G.L.Chen, P.J. McHugh, J.K. Tien, *Scripta Metall.*, **16** (1982) 483.
27. H. Burt, J.P. Dennison, B. Wilshire, *Metal Science*, **13** (1979) 295.
28. R. Lagneborg, B. Bergman, *Metal Science*, **10** (1976) 20.
29. W.J. Evans, G.F. Harrison, *Metal Science*, **10** (1976) 307.
30. C.R. Barrett, O.D. Sherby, *Trans. Met. Soc. AIME*, **233** (1965) 1116.
31. H.E. Evans, G. Knowles, *Acta Metall.*, **25** (1977) 963.
32. H.E. Evans, G. Knowles, Strength of Metals and Alloys, eds. P. Haasen et al., (Oxford: Pergamon Press, 1979), 301.
33. A.P. Miodownik, X. Li, N. Saunders, J.-P. Schille, *Parsons 2003: Engineering Issues in Turbine Machinery, Power Plant and Renewables,* eds. A. Strang et al., (London: Inst.MMM, 2003), 779.
34. A.P. Miodownik, *CALPHAD*, **2** (1978) 207.
35. W.J. Evans, G.F. Harrison, *Metal Science*, **13** (1979) 641.
36. R.W. Lund, W.D. Nix, *Acta Met.*, **24** (1976) 469.
37. G.B. Thomas, T.B. Gibbons, in Superalloys 1980, eds. J.K. Tien et al., TMS, 1980, 699.
38. O. Ajaja, T.E. Howson, S. Purushothaman, J.K. Tien, *Mater. Sci. Eng.*, **44** (1980) 165.
39. H.L. Eiselstein, D.J. Tillack, in Superalloys 718, 625 and Various Derivatives, ed. E.A. Loria, TMS, 1991, 1.
40. Special Metals Product Handbook of High-Peformance Alloys, Publication No. SMC-035, Huntington, WV: Special Metals Corporation, 2001.
41. S. Zhao, X. Xie, G.D. Smith, S.J. Patel, *Mater. Sci. Eng. A*, **A355** (2003) 96.
42. F. Tancret, T. Sourmail, M.A. Yescas, R.W. Evans, C. McAleese, L. Singh, T. Smeeton, H.K.D.H. Bhadeshia, *Mater. Sci. Technol.*, **19** (2003) 296.